RSC Applied Interfaces

ROYAL SOCIETY OF CHEMISTRY

COMMUNICATION

View Article Online
View Journal | View Issue

Cite this: *RSC Appl. Interfaces*, 2025, **2**, 634

Received 29th December 2024,
Accepted 24th February 2025

DOI: 10.1039/d4lf00423j

rsc.li/RSCApplInter

Reaction-passivation-driven delamination of spent $LiFePO_4$ cathodes and their upgrading to highly efficient catalysts for hydrogen evolution†

Jia Yi,[ab] Jinsong Hu,*[ab] Cheng Gong,[b] Qilong Liu [b] and Wentuan Bi *[ab]

2-Hydroxyphosphonic acid (HPAA) was demonstrated to delaminate spent $LiFePO_4$ cathodes from Al foil *via* a reaction-passivation mechanism, resulting in ultra-high-purity products and facilitating subsequent upgrading. As a proof of concept, Fe_x-P catalysts prepared from lithium-extracted $FePO_4$ slag deliver a hydrogen evolution current density of 10 mA cm^{-2} at an overpotential of only 88 mV.

Lithium-ion batteries (LIBs) have been widely used in consumer electronics and electric vehicles due to their high energy density, long cycle life, and minimal self-discharge.[1–3] The increasing demand not only drives rapid growth in the LIB industry, but also means that the number of spent batteries will increase significantly in the future.[4,5] In view of this trend, LIB recycling technologies, which not only help reduce the dependence on finite natural resources and therefore lower the costs, but also reduce the risk of environmental pollution, has become particularly urgent.[6] Therefore, establishing a cost-effective and eco-friendly recycling system is essential for the sustainable development of the LIB industry.[7]

To date, commercial recycling technologies generally use direct crushing, which mixes electrode materials with current collectors during processing, leading to higher energy consumption and pollution.[8] Pre-separation of these components is expected to alleviate the above problems.[9] The cathode, which is the main concern of battery recycling, is composed of cathode materials and conductive carbon strongly adhered to Al foil by a polyvinylidene fluoride (PVDF) binder.[10] How to efficiently delaminate the spent cathode materials from Al foil is crucial yet challenging. It has been proven that solvents such as *N*-methyl-2-pyrrolidone (NMP),[11] Cyrene,[12] deep eutectic solvents,[13,14] *etc.*, can dissolve the PVDF binder. However, due to the limited solubility of PVDF in these solvents, a large amount of solvent is often required, and the process is typically carried out under heating and mechanical agitation to achieve effective separation.[15] For the above reasons, exploring green and efficient alternative solvents has received widespread attention.[16,17]

In this study, we demonstrate a reaction-passivation strategy for the eco-friendly and efficient delamination of spent $LiFePO_4$ cathodes from Al foil. As illustrated in Fig. 1, HPAA can penetrate the cathode electrode sheets through the edges or cracks and form a dense passivation layer on the surface of the Al foil, which not only inhibits further reactions but also reduces the interaction between the Al foil and the binder. This strategy enables the separation of $LiFePO_4$ materials and Al foil with ultra-high purity, thereby facilitating subsequent upgrading. As a proof of concept, Fe_xP catalysts prepared from lithium-extracted $FePO_4$ slag show excellent hydrogen evolution activity, requiring 88 mV to achieve a current density of 10 mA cm^{-2} in 0.5 M H_2SO_4, which is superior to most reported iron phosphide catalysts. This research provides a feasible solution for the recycling and upgrading of spent $LiFePO_4$ cathodes.

HPAA, an excellent corrosion inhibitor, is chosen because of its strong chelating ability even in an acid or alkali. We first evaluated the effect of the concentration and pH of the HPAA

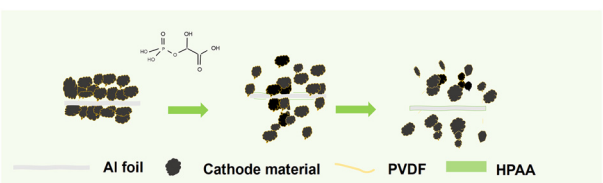

Fig. 1 Schematic illustration of the direct delamination of spent $LiFePO_4$ cathodes from the Al foil with the assistance of HPAA.

[a] *School of Chemical and Blasting Engineering, Anhui University of Science and Technology, Huainan 232001, PR China. E-mail: hujinsong1982@126.com, bwin@ustc.edu.cn*
[b] *Institute of Energy, Hefei Comprehensive National Science Center, Hefei, Anhui, 230031, P. R. China*

† Electronic supplementary information (ESI) available. See DOI: https://doi.org/10.1039/d4lf00423j

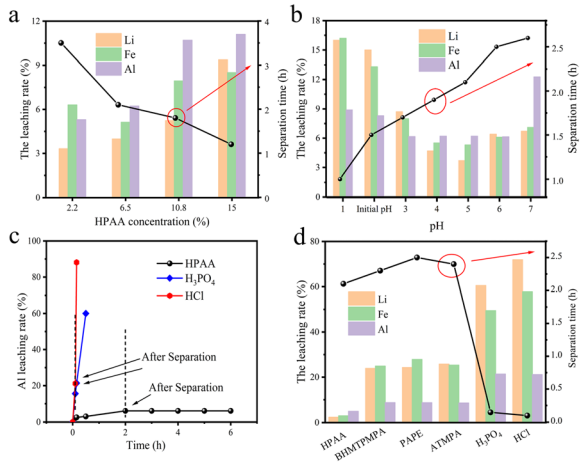

Fig. 2 (a) The concentration and (b) pH of HPAA aqueous solution on the separation efficiency and metal leaching rate. (c) Time-dependent leaching rates of Al in HPAA, HCl and H_3PO_4. (d) Comparison of different agents on the delamination of spent $LiFePO_4$ cathodes.

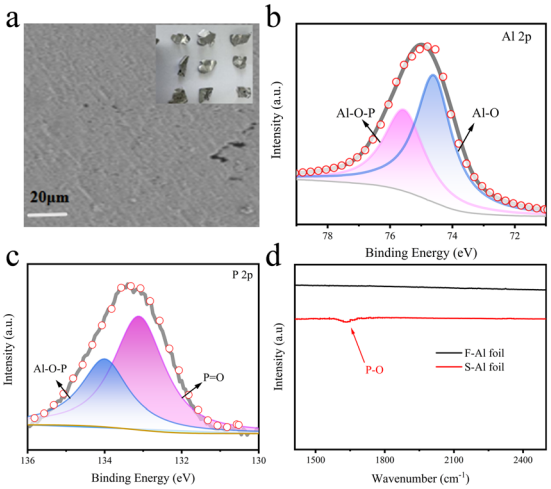

Fig. 3 (a) The SEM image of the Al foil after HPAA treatment and the inset is a photograph of the delaminated Al foils. High resolution XPS spectra of (b) Al 2p and (c) P 2p. (d) FTIR analysis.

aqueous solution on the separation efficiency and the metal leaching rate. As shown in Fig. 2a, the leaching rate of all the metals increased correspondingly with the increasing amount of HPAA. However, the separation efficiency showed the opposite trend. Taking both of the separation efficiency and the metal leaching rate into consideration, the concentration of 6.5 vol% was selected as the optimal condition for subsequent experiments. Furthermore, we adjusted the pH of the HPAA solution and evaluated their impact. According to the results in Fig. 2b, the leaching rates of Li and Fe were highest at the pH of 1, and gradually decreased as the pH increased. When the pH increased to 5, the leaching rates of all elements reached their lowest values. However, at the pH of 7, the leaching rate of Al increased dramatically, reaching its highest value. Based on these findings, the pH of 5 was selected as the optimal condition for the HPAA-assisted separation process, which achieved rapid delamination while minimizing the leaching of metals, thus ensuring the high efficiency and selectivity of the leaching process.

The Al leaching rate was monitored over time during the HPAA-assisted separation process. It is noteworthy that the leaching of Al ceased to increase after 2 hours, while it continued to increase in HCl and H_3PO_4. We also compared the influence of different organic acids on the separation efficiency of Al foil and cathode materials (Fig. 2d). The other three representative phosphonic acids: amino tri(methylene phosphonic acid) (ATMPA), polyhydric alcohol phosphate ester (PAPE), and bis-1,6-hexamethylenetriamine penta (methylene phosphonic acid) (BHMTPMPA) were also evaluated. The Al leaching rate was maintained at a low level, all less than 10% in the presence of phosphonic acids, with the lowest rate of 6.231% for HPAA.

To investigate the separation mechanism of spent $LiFePO_4$ cathode sheets in the presence of HPAA, X-ray photoelectron spectroscopy (XPS) was used to analyse the changes of chemical composition on the Al foil surface (Fig. 3a) and the inset is a photograph of the delaminated Al foils. The high resolution XPS spectra of Al 2p and P 2p (Fig. 3b–c) revealed characteristic peaks of Al–O–P on the surface of the Al foil, indicating the coordination interaction between Al^{3+} and the phosphonic functional group. Additionally, the FTIR spectrum of HPAA-treated Al foil (S-Al foil) displayed a new stretching vibration peak at 1641 cm^{-1} (Fig. 3d), compared to raw Al foil (F-Al foil), which corresponds to the characteristic absorption of P–O bonds. This indicates the formation of a dense Al–O–P layer on the surface of the Al foil. The formation layer supports the hypothesis that HPAA initially reacted with the Al foil to form a dense passivation layer on the surface, which effectively inhibited further corrosion and reduced the interaction between the Al foil and the binder, thereby promoting separation. This mechanism reveals the crucial role of HPAA in the direct delamination of spent $LiFePO_4$ cathodes.

To date, hydrometallurgical extraction of lithium is the main method for spent $LiFePO_4$ LIB recycling. However, the $FePO_4$ slag after lithium extraction is almost useless, causing a lot of waste and environmental problems.[18–20] Given that phosphides possess unique crystal and electronic structures, we have successfully upgraded the lithium-extracted $FePO_4$ slag to a Fe_xP catalyst *via* a thermal reduction process (Fig. S1†), demonstrating a proof of concept for LIB recycling and resource reutilization. The XRD pattern in Fig. S2† reveals that the upgraded material presents a composite phase of FeP and Fe_2P. In addition, to further improve the dispersion and conductivity of the catalyst, we also added graphene to the precursor and named the products $Fe_xP/G(x)$, where x in $G(x)$ represents the amount of graphene, as detailed in the ESI.† Detailed morphological and microstructural features of $Fe_xP/G(10)$ were investigated by high-resolution transmission electron microscopy (HRTEM) and elemental mapping. As shown in Fig. S3a,† Fe_xP particles with the size of about 100 nm and their aggregates are distributed on the surface graphene. The HRTEM image (Fig. S3b†) showed lattice fringes of 0.154 nm and 0.34

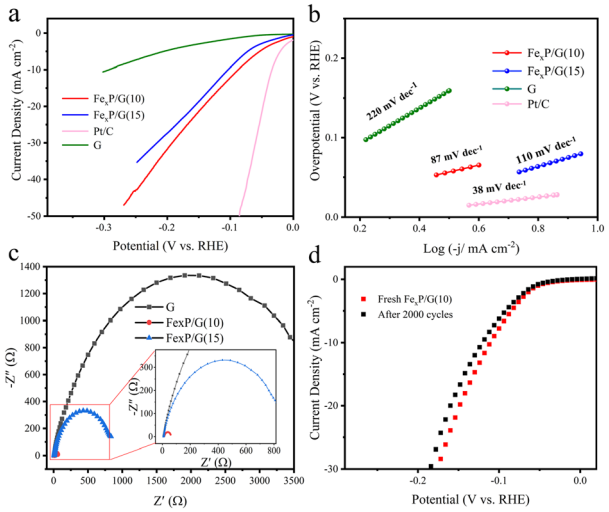

Fig. 4 HER performance. (a) LSV curves. (b) Tafel plots derived from LSV curves. (c) EIS. (d) The LSV curves before and after the durability test.

nm, corresponding to the (020) plane of FeP and the (001) plane of Fe_2P, respectively, consistent with the XRD result. The elemental mapping also revealed the distribution of the Fe, P and C elements in Fe_xP/G(10) (Fig. S4†).

The hydrogen evolution reaction (HER) from water electrolysis holds great promise for acquiring clean and renewable hydrogen energy. Thus, we evaluated the HER activity of the upgraded materials. As depicted in Fig. 4a, Fe_x-P/G(10) needs an overpotential of only 88 mV to deliver a current density of 10 mA cm^{-2} in 0.5 M H_2SO_4, which is superior to most reported iron phosphide catalysts (Table S1†). In addition, the HER kinetics was investigated through Tafel slope and electrochemical impedance spectroscopy (EIS). As shown in Fig. 4b, the Tafel slope of Fe_xP/G(10) is 87 mV dec^{-1}, indicating the Volmer–Heyrovsky mechanism. Additionally, Fe_xP/G(10) exhibits the smallest semicircle radius among all the synthesized materials in EIS (Fig. 4c), verifying its faster electron transfer rate during the HER process, and the corresponding equivalent electrical circuit is shown in Fig. S5.† The double-layer capacitance (C_{dl}) was used as an indicator to evaluate the electrochemical active surface area of the catalysts. As illustrated in Fig. S6,† Fe_xP/G(10) exhibited the largest C_{dl} of 3.87 mF cm^{-2} among the three samples, indicating the enhanced electrochemically active surface area. Fig. 4d shows that the overpotential at 10 mA cm^{-2} of Fe_xP/G(10) increased by only 9 mV after 2000 cycles of cyclic voltammetry tests. Moreover, it can maintain a stable current density of about 10 mA cm^{-2} for more than 20 h without obvious fluctuations (Fig. S7†), demonstrating the outstanding durability of the upgraded catalyst. Thus, the results confirmed that the synthesized Fe_xP catalyst, upgraded from the spent $LiFePO_4$, holds great potential for HER applications.

The reaction-passivation strategy enables the separation of cathode materials and Al foil with ultra-high purity, representing a promising strategy for recycling LIB materials. The delamination and upgrading processes might be adaptable to large-scale recycling of spent $LiFePO_4$ cathodes, providing a scalable method for producing HER catalysts.

This work was financially supported by the National Natural Science Foundation of China (22175051), and the Institute of Energy, Hefei Comprehensive National Science Center (22KZS401, 22KZL401, 21KZZ510).

Data availability

The data supporting this article have been included as part of the ESI.†

Conflicts of interest

There are no conflicts to declare.

Notes and references

1 F. M. N. U. Khan, M. G. Rasul, A. S. M. Sayem and N. K. Mandal, *J. Energy Storage*, 2023, **71**, 108033.
2 M. B. F. Ahsan, S. Mekhilef, T. K. Soon, M. b. Mubin, P. Shrivastava and M. Seyedmahmoudian, *Int. J. Energy Res.*, 2022, **46**, 19826–19854.
3 Y. Bai, R. Essehli, C. J. Jafta, K. M. Livingston and I. Belharouak, *ACS Sustainable Chem. Eng.*, 2021, **9**, 6048–6055.
4 V. Nguyen-Tien, Q. Dai, G. Harper, P. A. Anderson and R. J. R. Elliott, *Appl. Energy*, 2022, **321**, 0306–2619.
5 E. Fan, L. Li, Z. Wang, J. Lin, Y. Huang, Y. Yao and F. Wu, *Chem. Rev.*, 2020, **120**, 7020–7063.
6 C. M. Costa, J. C. Barbosa, R. Gonçalves, H. Castro, F. J. D. Campo and S. Lanceros-Méndez, *Energy Storage Mater.*, 2021, **37**, 433–465.
7 J. J. Roy, S. Rarotra, V. Krikstolaityte, K. W. Zhuoran, Y. D.-I. Cindy, X. Y. Tan, M. Carboni, D. Meyer, Q. Yan and M. Srinivasan, *Adv. Mater.*, 2022, **34**, 2103346.
8 G. Harper, R. Sommerville, E. Kendrick, L. Driscoll, P. Slater, R. Stolkin, A. Walton, P. Christensen, O. Heidrich, S. Lambert, A. Abbott, K. Ryder, L. Gaines and P. Anderson, *Nature*, 2019, **575**, 75–86.
9 H. Bae and Y. Kim, *Mater. Adv.*, 2021, **2**, 3234–3250.
10 W. Zhang, C. Xu, W. He, G. Li and J. Huang, *Waste Manage. Res.*, 2018, **36**, 99–112.
11 H. Zhou, B. Pei, Q. Fan, F. Xin and M. S. Whittingham, *J. Electrochem. Soc.*, 2021, **168**, 040536.
12 T. Marino, F. Galiano, A. Molino and A. Figoli, *J. Membr. Sci.*, 2019, **580**, 224–234.
13 M. Wang, Q. Tan, L. Liu and J. Li, *ACS Sustainable Chem. Eng.*, 2019, **7**, 12799–12806.
14 Y. Bai, M. Li, C. J. Jafta, Q. Dai, R. Essehli, B. J. Polzin and I. Belharouak, *Sustainable Mater. Technol.*, 2023, **35**, e00542.
15 R. a. Li, M. Li, Z. Liu and Y. Cao, *Chem. Commun.*, 2022, **58**, 13975–13978.
16 J. Neumann, M. Petranikova, M. Meeus, J. D. Gamarra, R. Younesi, M. Winter and S. Nowak, *Adv. Energy Mater.*, 2022, **12**, 2102917.

17 Y. He, X. Yuan, G. Zhang, H. Wang, T. Zhang, W. Xie and L. Li, *Sci. Total Environ.*, 2021, **766**, 142382.
18 C. Yang, M. Zhao, C. Zhang, S. Zhang, D. Zhu and C. Guo, *Chem. Commun.*, 2025, **61**, 141.
19 A. Flambard, L. Montagne and L. Delevoye, *Chem. Commun.*, 2006, **32**, 3426–3428.
20 A. Baby, D. Singh, C. Murugesan and P. Barpanda, *Chem. Commun.*, 2020, **56**, 8400–8403.